International Journal of Applied Mathematics

Volume 38 No. 11s 2025,

ISSN: 1311-1728 (printed version); ISSN: 1314-8060 (on-line version)

DC-CNN-SE: A DEEP CONVOLUTIONAL CAPSULE NETWORK WITH SQUEEZE-AND-EXCITATION AND BAYESIAN LEARNING FOR MULTI-MODAL MRI BRAIN TUMOR CLASSIFICATION

Manjari Joshi[a], A. K. Pal[a*], Ankita Pandey[b]

[a]Department of Mathematics, Statistics & Computer Science, Govind Ballabh Pant University of Agriculture and Technology, Pantnagar-263145, Uttarakhand, India, 59785@gbpuat.ac.in, arun_pal1969@yahoo.co.in

[b]Department of Mathematics, Institute of Applied Sciences and Humanities, GLA University Mathura, 281406, UP, India, Ankitapandey0595@gmail.com

Abstract:

The classification and segmentation of brain tumors in multi-modal MRI scans are highly complex tasks due to variations in shape, size, and appearance across different imaging modalities. This paper presents a novel Deep Convolutional Capsule Neural Network with Squeeze-and-Excitation (DC-CNN-SE) blocks, incorporating a Bayesian uncertainty module and prototype-guided representation learning for classifying brain tumors in multi-modal MRI. By combining T1, T2, T1C, and FLAIR images, our model uses squeeze-and-excitation blocks to recalibrate feature maps, emphasizing modality-specific tumor features. Additionally, a Bayesian uncertainty quantification mechanism provides reliable prediction confidence estimates, addressing clinical concerns about misclassification. Moreover, a prototype-guided representation learning approach is included to improve the separability of features in the latent space, boosting generalization across patients. The architecture, enhanced with deep convolutional layers, Leaky ReLU activations, batch normalization, and dropout, achieves excellent performance on the BraTS2020 dataset, with accuracy (99.00%), precision (98.95%), recall (98.91%), F1-score (98.90%), MCC (98.65%), and CSI (97.84%) metrics are used for segmentation and classification of MR Images. This framework marks a significant step forward in clinical decision-making for brain tumor diagnosis. Both qualitative and quantitative results demonstrate that our proposed model is effective and surpasses current state-of-the-art (SOTA) methods.

* https://www.med.upenn.edu/cbica/brats2020/

Math Subject Classification 2020: 68T07 Artificial neural network and deep learning.

Keywords: Multi-modal, Classification, DC-CNN (Deep Convolutional Capsule Neural Network), MRI, SE (Squeeze-and-Excitation), Bayesian uncertainty module.

1. Introduction

To a large extent, the early detection of brain tumors ensures proper management and improves the prognosis for the patient. MRI continues to be the gold standard in the diagnosis

Received: August 06, 2025

Volume 38 No. 11s 2025,

ISSN: 1311-1728 (printed version); ISSN: 1314-8060 (on-line version)

of brain tumors, providing exquisite details of localization, size, and nature of the tumor. However, the various appearances of tumors in different imaging modalities and the natural anatomy of the brain make proper segmentation and classification a challenging task. Applications of multi-modal MRI data, such as T1, T2, T1C, and FLAIR scans, contain rich information, but there lie several problems encountered with the process of effective feature extraction and integration [1-2]. Traditional tasks for brain tumor manual segmentation are time-consuming and prone to large inter- and intra-observer variability; therefore, more accurate automated methods are needed [3-4]. Although the traditional machine learning algorithms and simple CNNs had encouraging preliminary results in this area, they often fail to respect complex spatial hierarchies inherent in tumor structures [5]. Also, most of these methods fail to capitalize on the complementary information from different MRI modalities, which makes them perform less than optimally in clinical scenarios [6].

To address these drawbacks, we introduce a Deep Convolutional Capsule Neural Network with Squeeze-and-Excitation (DC-CNN-SE) blocks for multi-modal MRI brain tumor classification. In contrast to traditional CNNs, our model employs Squeeze-and-Excitation (SE) blocks to remodel channel-wise feature responses, thus improving modality-specific tumor features while eliminating redundant information [7]. Moreover, the introduction of Capsule Networks allows the model to capture spatial hierarchies and intricate geometric patterns of tumor areas that are usually neglected in conventional CNN approaches [8]. We also enhance model trustworthiness by Bayesian uncertainty estimation, with confidence values being critical to medical decision-making. Additionally, prototype-guided feature refinement guarantees intra-class cohesion and inter-class distinctness, resulting in resilient classification results. Together, these innovations make the proposed DC-CNN-SE approach a new and powerful solution for enhancing the accuracy and explainability of brain tumor classification tasks [9].

These challenges call for a novel Deep Convolutional Capsule Neural Network with a Squeeze-and-Excitation DC-CNN-SE framework with prototype-guided Bayesian learning. In such a manner, we integrate various innovations that help us effectively enhance the classification of brain tumors. The novel aspects of the given approach are summarized by the following points:

- Multi-Modal MRI Fusion: Integration of T1, T2, T1C, and FLAIR scans to capture complementary tumor-specific features, unlike single-modality approaches.
- SE Block Recalibration: Dynamic enhancement of informative tumor regions while suppressing irrelevant signals for better feature learning.
- Capsule Networks: Preservation of spatial hierarchies and tumor geometry, addressing CNN limitations in handling complex tumor structures.
- Bayesian Uncertainty Estimation: Confidence-aware predictions to improve clinical reliability and reduce misclassification risks.
- Introduced K-means clustering–driven feature refinement to enhance segmentation boundaries and guide prototype learning.

Received: August 06, 2025

International Journal of Applied Mathematics
Volume 38 No. 11s 2025,
ISSN: 1311-1728 (printed version); ISSN: 1314-8060 (on-line version)

- Prototype-Guided Representation Learning: Structured latent features for improved intra-class compactness and inter-class separability, ensuring robust generalization.

The DC-CNN-SE model is one of the latest additions in the sphere of brain tumor analysis, where novel techniques that lead to enhanced feature extraction are combined with their ability to improve accuracy in classification. Advanced Convolutional Layers Combined with Regularization Techniques: The architecture consists of advanced convolutional layers with Leaky ReLU activation that correct the problem of vanishing gradients and Batch Normalization for a fast convergence rate [10-11]. Using these algorithms along with dropout layers ensures high generalization and prevents the model from overfitting to the patient data while functioning well for different sets of patient data and also ensuring better improvement in the respective target variables, with less chance of overfitting, and thus enhances the model efficiently, as assured earlier [12]. Our framework exhibits the ability to facilitate clinical decision-making by correctly pointing out some of the most critical features of the tumor, thus leading to more reliable predictions and better patient outcomes. Our approach addresses the complexity of multi-modal data integration and preservation of spatial hierarchies, setting a new standard in brain tumor segmentation and classification [15-16].

2. Literature survey

In recent times, extensive work has been done on brain tumor identification and typing through deep learning as well as hybrid approaches to improve accuracy, stability, and computation speed. Early methods, including the adaptive region growing algorithm designed by Zikic et al. [1], formed the base for brain tumor segmentation on MRI. Nevertheless, the method suffered from its dependency on human intelligence and failure to deal with intricate tumor textures. To overcome these limitations, Isensee et al. [2] integrated segmentation strategies through the combination of radiomics-based survival prediction and the BRATS2017 challenge, showing that multi-task learning and feature extraction of tumor regions can enhance survival estimation.

Convolutional Neural Networks (CNNs) transformed medical image analysis, with classification, segmentation, and detection capabilities dominated by them. A review paper by Litjens et al. [3] summarized the stunning success of CNNs, while also conceding that overfitting, generalization, and small medical datasets posed some issues. To counter these issues, Albarqouni et al. [4] proposed the use of batch-specific focal loss to focus on the most difficult samples to classify, essentially enhancing CNN performance for detecting small tumors—a very relevant aspect in medical imaging. Bakas et al. [5] expanded on previous expert models by supplementing The Cancer Genome Atlas glioma MRI datasets with expert segmentation labels and radiomic features, providing more accurate training data. From a technical standpoint, Jha et al. [6] surveyed some of the deep learning techniques for brain tumor segmentation and found Capsule Networks (CapsNet) [26] to be a prospective method for maintaining spatial relationships, which is an important consideration in proper tumor classification. CapsNet, as shown by Sabour et al. [8], was found to be a strong competitor to CNNs in medical image processing because it could represent spatial hierarchies.

Received: August 06, 2025

Volume 38 No. 11s 2025,

ISSN: 1311-1728 (printed version); ISSN: 1314-8060 (on-line version)

Simultaneously, Hu et al. [7] investigated Squeeze-and-Excitation (SE) Networks to recalibrate features, greatly enhancing the performance of segmentation by focusing on task-relevant features and distracting from less informative information. Regularization strategies like batch normalization [9], and dropout [10], became the norm in avoiding overfitting and increasing the generalization ability of the model, particularly in the context of medical datasets.

Optimization algorithms also changed, most significantly with the AdamW optimizer proposed by Loshchilov & Hutter [11], which includes weight decay regularization to increase model training. Hybrid strategies have also further enhanced performance: Gumaei et al. [17] merged hybrid feature extraction with regularized ELM for increased classification accuracy, whereas Özyurt et al. [18] combined fuzzy C-means clustering with CNN-ELM for better segmentation and classification. Li et al. [19] put forth a multi-modal information fusion approach, combining T1, T2, and FLAIR images to improve robustness and minimize variability between imaging modalities. New optimization methods, including the Whale Harris Hawks algorithm of Rammurthy & Mahesh et al. [20] and blockchain-based deep CNNs of Mohammad et al. [21], are examples of merging state-of-the-art optimization and secure computing in medical imaging. Transfer learning has also emerged as a priceless addition for better classification performance. Rehman et al. [22] introduced a deep learning model for brain tumor automatic classification based on transfer learning, with enhanced performance on small datasets.

Later, Chen Li et al. [23] proposed a hybrid method that involves parallel CNNs with Firefly optimization [31] and reported a testing accuracy of 98.40%. Haq et al. [30] (2022) suggested DACBT, a deep learning-based method for classifying brain tumors in an IoT-supported healthcare system. Their proposal emphasizes the revolutionary power of real-time observation and decision-making in the healthcare system with deep learning and IoT integration, with high accuracy, recall, and precision on MRI datasets. Huang et al. [33] introduced a new model that integrates CNN and transformer networks to enhance the segmentation of brain tumors on various MRI types. Their approach helped in getting better results even when some images are unclear or missing. But the main drawback of this study is that the model is very complex and needs high computer power, which makes it hard to use in real-time or low-resource setups. Li et al. [34] advocated for an importance-aware 3D visualization system for medical image retrieval, which enhances diagnostic appropriateness, but not with deep segmentation integration. Feng et al. [35] designed an AR-based 3D tumor visualization system, increasing interactivity but depending on manual segmentation, which restricts automation. Islam et al. [36] designed Sofnet for slice augmentation based on optical flow, enhancing generalization to MRI datasets but ignoring inter-modality fusion and spatial coherence.

Deep learning innovations have greatly enhanced automated brain tumor classification and grading from MRI images. Zheng et al. [37] introduced UniVisNet, a unified visualization and classification network where feature representation and decision-making are combined into one system for glioma grading. The method showed higher accuracy through the joint optimization of visualization and classification tasks, enabling it to identify subtle tumor-

Received: August 06, 2025

Volume 38 No. 11s 2025,

ISSN: 1311-1728 (printed version); ISSN: 1314-8060 (on-line version)

specific features. Similarly, Aamir et al. [38] proposed a framework for MRI-based brain tumor classification using deep learning, demonstrating how convolutional architectures can effectively learn discriminative features from complex tumor patterns. Their work highlighted the clinical usefulness of automatically categorizing tumors to assist radiologists. In another study, Huang et al. [39] introduced a CNN model incorporating complex network theory and a new activation function, which improved feature extraction and classification accuracy on brain tumor datasets. Collectively, these studies reveal an emerging trend of adapting CNN architectures with novel modules, activation functions, and optimization techniques to enhance tumor detection and classification, emphasizing deep learning's potential for reliable clinical decision support in neuro-oncology.

In brief, during 2014-2024, significant developments in the detection and classification of brain tumors, as illustrated in Table 1, have been achieved. These developments include adaptive segmentation techniques, improved CNN architectures, combination models, and advanced optimization algorithms. The fusion of deep learning and machine learning techniques continues to improve accuracy and performance, with CapsNet and SE Networks presenting improvements in feature learning and extraction. Therefore, medical image analysis is presently better positioned to deal with issues of spatial hierarchies, intricate tumor anatomy, and class imbalance. However, there are challenges. Such models as CNNs and CapsNet are still prone to overfitting and consume huge computational power and large datasets. Although SE Networks enhance feature learning, deeper architectures and hybrid solutions need investigation. In this paper, we introduce enhancing the DC-CNN structure through the incorporation of SE mechanisms to better enhance feature representation and spatial preservation with lower computational complexity. This approach is anticipated to enhance accuracy in the processing of imbalanced datasets and enhance detection performance for small tumors as rendered in MRI images.

3. Methodology

This study begins by outlining the specifications of the dataset utilized for brain tumor classification in MRI images. Following that, it details the sequential steps involved in the proposed method for classifying brain tumors. Each stage of the process, from data handling to model implementation, is systematically presented to provide a clear understanding of the methodology employed in this research.

3.1 Dataset

The BRATS 2020[29] dataset for the Brain Tumor Segmentation Challenge is made available in the framework of 367 MRI images in each of four types of modalities; these modalities include T1, T2, T1C, and FLAIR. A modality is the capture of different aspects of anatomy and pathology needed in the brain to embrace a holistic study of the tumors. In detail, a T1 image represents the structural anatomy, T2 images emphasize edema, T1C enhances the visualization of tumors, and FLAIR suppresses the fluid signals with enhanced detection of the lesions. Ground truth annotations comprised another part of the dataset, as they are crucial for evaluating machine learning models in terms of outlined regions of tumors, including the

Received: August 06, 2025

Volume 38 No. 11s 2025,

ISSN: 1311-1728 (printed version); ISSN: 1314-8060 (on-line version)

enhancing tumors, i.e., ET, and tumor cores, referring to TC. Pre-processing resized images of the same size - 224x224 pixels for the DC-CNN-SE model, and normalized pixel values to be within the range [0, 1]. One-hot encoding for multi-class classification for the labels, and then the training and testing sets are split in an 80/20 ratio. Data augmentation has also been performed to make the model even stronger in terms of robustness.

3.2 Introduced Framework

In this paper, we introduced a novel approach for processing multi-modal MRI images and classification of these MRI images, which combines Optimization, segmentation techniques, and deep learning, and includes the following steps in Fig.1(a) and Fig.1(b).

1. Data preprocessing and Data augmentation
2. Segmentation of multi-modal MRI region
3. Classification using DC-CNNN-SE with Bayesian dropout
4. Model optimization and evaluation
5. Feature refinement via K-means clustering
6. Visualization of outcomes

Table 1. Summary of Research on Models for the Identification of Brain Tumors.

Reference	Year	Authors	Key findings	Challenges
1	2014	Zikic et al.	Adaptive Region Growing Technique Laid groundwork for brain tumor segmentation in MRI; relied on human intervention and struggled with complex tumor structures.	Dependence on human intervention; difficulty handling complex tumor textures.
10	2014	Loshchilov & Hutter et al.	AdamW Optimizer Improved CNN training stability and performance through built-in weight decay regularization.	Adapting to different datasets requires fine-tuning of learning rate & decay parameters.
9	2015	Ioffe & Szegedy et al.	Batch Normalization Accelerated training and improved model generalization, are crucial for medical datasets.	Require careful parameter tuning; inappropriate use can lead to diminished model performance.
4	2016	Albarqouni et al.	Focal Loss Technique Improved CNN performance in detecting small tumors by focusing on	Class imbalance remains a challenge; and requires careful

Received: August 06, 2025

Volume 38 No. 11s 2025,
ISSN: 1311-1728 (printed version); ISSN: 1314-8060 (on-line version)

			difficult-to-classify samples to address class imbalance.	tuning of loss function parameters.
2	2017	Isensee et al.	Multi-task Learning with Radiomics combined segmentation and survival prediction, enhancing survival rate estimation from tumor feature extraction.	Multi-task learning complexity; potential for overfitting due to multiple objectives.
3	2017	Litjens et al.	Comprehensive Review of CNNs Highlighted the successes of CNNs in classification, segmentation, and detection; identified issues of overfitting and generalization.	Generalization issues; risk of overfitting due to limited medical data.
8	2017	Sabour et al.	Capsule Networks (CapsNet) Addressed the limitations of CNNs by encoding spatial hierarchies, improving medical image processing.	CapsNet architectures can be more complex; training can be resource-intensive.
5	2018	Bakas et al.	Enhanced Cancer Genome Atlas Glioma MRI Collection Improved dataset with expert segmentation labels and radiomic features for better model training.	Data quality issues; reliance on expert annotations can lead to variability in labeling.
7	2018	Hu et al.	Squeeze-and-excitation (SE) Networks Enhanced attention to important features in tumor segmentation, improving overall model performance.	Computational complexity; increased model size may require more resources for training and inference.
6	2019	Jha et al.	Review of Deep Learning Methods Identified Capsule Networks (CapsNet) as a promising method for preserving spatial relationships in tumor classification.	Limited awareness and understanding of CapsNet among researchers; requires further validation.
17	2019	Gumaei et al.	Hybrid Feature Extraction with Regularized Extreme Learning Machines (ELM) Increased	The complexity of hybrid approaches can make

Volume 38 No. 11s 2025,
ISSN: 1311-1728 (printed version); ISSN: 1314-8060 (on-line version)

			classification accuracy on brain tumor datasets.	implementation challenging; and requires careful integration.
19	2019	Li et al.	Multi-modal Information Fusion Framework Utilized multiple MRI modalities (T1, T2, FLAIR) to improve robustness and minimize variability in classification outcomes.	Variability in image quality across modalities; integration complexity may hinder processing speed.
18	2020	Özyurt et al.	Hybridization of Fuzzy C-Means Clustering with CNN-ELM Enhanced segmentation and classification accuracy in tumor detection.	Balancing accuracy and computational efficiency can be difficult; reliance on fuzzy logic may complicate outcomes.
22	2020	Rehman et al.	Transfer Learning Framework Enabled pre-trained models to adapt quickly to brain tumor datasets, improving performance with limited data.	Adapting pre-trained models can sometimes lead to suboptimal performance on specific tasks.
21	2021	Mohammad et al.	Blockchain-based Deep CNNs ensured secure and accurate brain tumor predictions using advanced computing techniques.	Complexity in implementing blockchain technology and potential scalability issues.
20	2022	Rammurthy & Mahesh et al.	Whale Harris Hawks Optimization Algorithm. Implemented deep optimization techniques for more accurate brain tumor predictions.	Limited real-world application; requires robust validation on diverse datasets.
30	2022	Haq et al.	The proposed methodology increases brain tumor classification accuracy in IoT healthcare	NA

Received: August 06, 2025

International Journal of Applied Mathematics
Volume 38 No. 11s 2025,
ISSN: 1311-1728 (printed version); ISSN: 1314-8060 (on-line version)

23	2024	Chen Li et al.	Parallel CNNs with Firefly Optimization achieved a testing accuracy of 98.40% in the segmentation and classification of MRI images.	The complexity of parallel architecture may increase computational load and require efficient resource management.
33	2024	Huang, Wei, Zhang, Zhang	Combined CNN and transformer-based techniques for improved segmentation on multi-modal MRI data.	High model complexity requires significant computational resources, hindering practical deployment.

3.3 Pre-processing and Data Augmentation

Pre-processing is one of the important phases in the process, such that the data is adequately prepared for deep learning models. For brain tumor classification using MRI images, pre-processing involves several crucial steps. These steps are taken to standardize and enhance the dataset for effective model training. MRI images are scanned differently in dimensions, so to establish uniformity, resize all the images to 224×224 pixels. This resampling ensures that the model treats inputs uniformly and saves computation. After re-sampling, image normalization is applied: the pixel values are scaled to the interval [0,1], [0,1], and [0,1]. Because pixel values would be in the range 0 to 255, scaling by 1/255 helps alleviate the problem of exploding gradients in early training. Mathematically, the normalized image looks like:

$$I' = \frac{I}{255} \quad (1)$$

Where I = original pixel intensity

I' = Normalized pixel intensity

This is because categorical labels describing types of tumors have to be explicitly converted into numerical forms so that the model may process the data appropriately. This encoding begins with Label Encoding, whereby string labels such as "Glioma," "Meningioma," and "Pituitary" are mapped uniquely into integer values. For example, one can assign 0 to "Glioma", 1 to "Meningioma", and 2 to "Pituitary". Using this sort of numerical encoding, a model can treat each category as a separate class. label encoding comes with another important step: One-Hot Encoding, which is currently considered significant in multi-class classification problems. One-hot encoding converts the integer labels into a binary vector, where each class

Received: August 06, 2025

Volume 38 No. 11s 2025,

ISSN: 1311-1728 (printed version); ISSN: 1314-8060 (on-line version)

is represented by one vector with zeros everywhere except for one place at the class index of the label. So "Glioma" (label 0) becomes [1, 0, 0], "Meningioma" (label 1) becomes [0, 1, 0], and "Pituitary" (label 2) becomes [0, 0, 1]. This format ensures the model is not assuming some ordinal relationship between the different types of tumors, thus allowing the model to distinguish between them. Through the conversion of labels into binary vectors, the model is effective in the classification tasks in a structured and interpretable manner.

Fig.1(a) .Block diagram of the proposed method.

To address potential class imbalance and prevent overfitting, we employed an extensive data augmentation technique using the KerasImageDataGenerator module. The data augmentation pipeline included the following transformations:

- **Rotation:** Applied a rotation of $\theta = 20^0$ To ensure that the model can process images with small orientation differences. The mathematical expression for rotation is given below:

$$\begin{bmatrix} X' \\ Y' \end{bmatrix} = \begin{bmatrix} \cos(20) & -sin(20) \\ sin(20) & cos(20) \end{bmatrix} \begin{bmatrix} X \\ Y \end{bmatrix} \quad (2)$$

Where X and Y are the original coordinates and X', Y' These are the transformed coordinates.

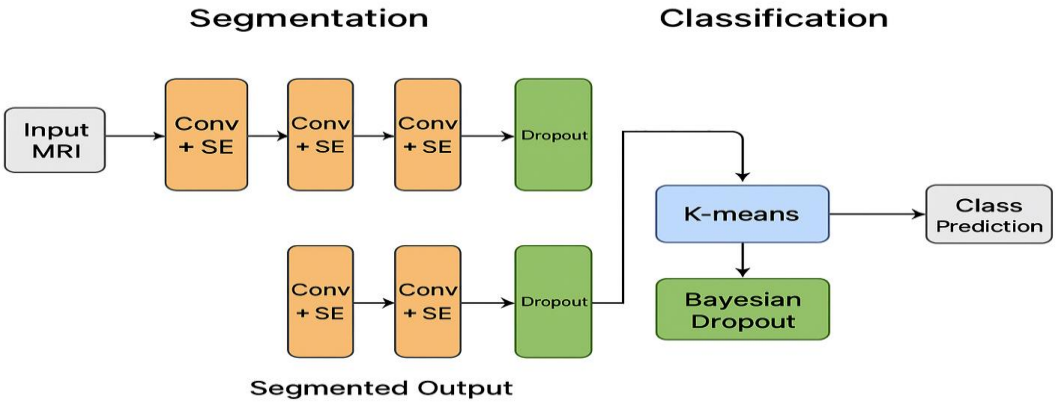

Fig. 1(b). flowchart of segmentation and classification for proposed method.

- **Zoom**: Applied a scale with a scale factor S_X =1.15 and S_Y=1.15, which helps the model learn scale-invariant features. The transformation is defined as:

$$(X', Y') = (1.15\,X, 1.15\,Y) \quad (3)$$

- **Width and height shifts**: applied a shift in both horizontal and vertical direction of 20% of the image size. Translation is given by:

$$(X', Y') = (X+0.2W, Y+0.2H) \quad (4)$$

Where W and H are the width and height of the images.

- **Shear transformation**: Applied a shear angle of 0.15 radian, simulating small distortion during MRI acquisition:

$$\begin{bmatrix} X' \\ Y' \end{bmatrix} = \begin{bmatrix} 1 & 0.15 \\ 0.15 & 1 \end{bmatrix} \begin{bmatrix} X \\ Y \end{bmatrix} \quad (5)$$

Received: August 06, 2025

International Journal of Applied Mathematics
Volume 38 No. 11s 2025,
ISSN: 1311-1728 (printed version); ISSN: 1314-8060 (on-line version)

All images are tagged using a Label Encoder and one-hot encoding to ensure compatibility with categorical cross-entropy loss during model training. They all enhanced the robustness and generalization of the model to unseen MR images, which is essential in medical imaging analysis.

3.4 Segmentation and Feature Extraction

Different transformations are applied to artificially increase the diversity of training images. Firstly, the image rotation step involves rotating the images by a random angle within a certain range. In mathematical expression, it uses a rotation matrix to enable the model to identify the tumor irrespective of the angle at which it presents. Then, width shifts and height shifts are done so that the image is moved within a horizontal or vertical axis based on the fraction of its size, so the model learns to point to tumors in a given region. Zooming is also implemented, which would enable images to be viewed at different distances, simulating closer or far away perspectives. Also, shearing slightly warps the images, which helps the model to identify stretched or tadpole-shaped tumors. Flipping horizontally and vertically ensures that the model learns invariant features from different orientations. Other than that, brightness adjustment is made to handle varying illumination by multiplying pixel values by a brightness factor. Finally, this normalization standardizes pixel values into the range of [0, 1] by normalizing pixels in the process and, hence, stabilizing training. Combining all these techniques, the training dataset becomes richer and more varied, hence better able to help the DC-CNN generalize well and lead to effectiveness in a task, such as tumor classification, detection, and segmentation.

In our proposed DC-CNN-SE method, segmentation and feature extraction take on the roles that truly enhance the identification of brain tumors from the MRI images. The proposed delineation of the boundary between the tumors in the brain scan is determined using CNNs. A set of learnable filters is applied for each convolutional layer of the CNNs to input images to capture key spatial features. This can be represented mathematically as follows:

$$h(I,j) = \sum_m \sum_n f(m,n).x(i+m,j+n) \quad (6)$$

Where f (m, n) represents the filter and x values of the input pixel. Non-linear activation functions are used, which in this paper are Leaky ReLU [25] it is the kind of activation function that enforces some nonlinear representation in the model to learn complex data patterns. Batch Normalization is made use of to stabilize the learning process by normalizing the activations of each layer - reducing internal covariate shift and allowing for faster convergence.

The most important modification of our model is the use of SE blocks, which are the feature map recalibration modules. These modules focus on amplifying the most relevant channels and eliminating irrelevant ones. Using mathematical expressions, the process is written as follows:

$$S = (W_2 .ReLU (W_1 .z)) \quad (7)$$

Received: August 06, 2025

International Journal of Applied Mathematics
Volume 38 No. 11s 2025,
ISSN: 1311-1728 (printed version); ISSN: 1314-8060 (on-line version)

Where S is the recalibrated feature map, **σ** is the sigmoid activation function, z is the globally pooled feature vector andW_1 , $W_2$are the learnable weights. SE blocks, in this manner, allow the network to focus more on the relevant features, hence improving segmentation accuracy. Segmentation performance is quantitatively assessed using Mean Structural Similarity (MSS) and Confusion Similarity Index (CSI) metrics, ensuring robust evaluation of boundary delineation and structural fidelity of tumor regions.

While GAP (global average pooling) reduces the spatial dimension of the feature maps, it conserves the crucial spatial information to preclude overfitting as well as correct classification, thus satisfying the later stages of a network. The synergy between DC-CNNs, SE blocks, and GAP produces a robust framework for tumor segmentation and feature extraction that could lift the ability of the model toward better classification with high sensitivity and specificity of brain tumors within MRI scans.

3.5 Classification using DC-CNN-SE with Bayesian dropout

In the proposed Deep Convolutional Capsule Neural Network with a Squeeze-and-Excitation model, classification plays a very important role in deciding what kind of tumor is present within the MRI images. In this, features extracted due to the segmentation and feature extraction are used to classify based on predictions during the classification phase. The GAP function is the first one in this process, as it lowers the spatial dimensions of feature maps but retains the relevant information useful for classification. Mathematically, GAP is written as:

$$y_k = \frac{1}{H \times W} \sum_{i=1}^{H} \sum_{j=1}^{W} x_{ij} \quad (k) \quad (8)$$

Where, y_k = output features of class k

H = height of the feature map, W = width of the feature map

This reduces feature maps to a single feature vector for every class as it collapses all the feature maps into one vector by class.

Once the dimensionality is reduced, a fully connected layer uses the pooled features to map them into class scores. Then, the output of this layer goes to the softmax layer, which computes the probability distribution over different classes of tumors. Mathematically, the definition of the softmax function is as follows:

$$P \quad (y= \quad c| \quad x) \quad = \quad \frac{e^{z_c}}{\sum_{i=1}^{C} e^{z_i}} \quad (9)$$

Where P (y= c| x) denotes the probability that the input x belongs to class c, C denotes the total number of classes,z_c denotes the logits of c. The softmax function normalizes the logits into a range between 0 and 1, enabling the model to express confidence in its predictions. The class with the highest probability is selected as the final prediction, thus ensuring the classification of the type of tumor is effective and reliable. Besides that, the model is trained using a

Received: August 06, 2025

International Journal of Applied Mathematics
Volume 38 No. 11s 2025,
ISSN: 1311-1728 (printed version); ISSN: 1314-8060 (on-line version)

Categorical Cross-Entropy Loss function for better predictive performance. This is defined as follows.

$$L=-\sum_{i=1}^{C} y_i \cdot \log(y'_i) \quad (10)$$

Where, y_i = true label, (y'_i) = Predicted probability for class i

In this loss function, the model measures the difference in dissimilarity between the true labels and their corresponding predicted probabilities to optimize prediction errors and improve the overall accuracy of a DC-CNN-SE model in classifying types of brain tumors. Through such streamlined systematic steps, the classification phase of the model ensures that the model can tell apart very different types of tumors, which leads to more accurate diagnosis and treatment. For reliable tumor categorization, we integrate Bayesian Dropout into dense layers for uncertainty-aware predictions and refine feature embeddings using K-Means clustering for improved class separability.

3.5.1 Bayesian Dropout for Uncertainty Estimation

Standard convolutional neural networks (CNNs) make deterministic predictions, which are not reliable in safety-critical applications, such as medical imaging. To overcome this limitation, we use Bayesian Dropout in dense layers of the classification head. In contrast to standard dropout, which is disabled at test time, Bayesian Dropout is always on during inference, allowing for several stochastic forward passes. This computation provides an approximation to a variational Bayesian posterior over the weights, yielding not only class probabilities but also predictive uncertainties. Uncertainty estimation like that is important for medical diagnosis, where overconfident misclassifications may have disastrous consequences.

Equation for Bayesian Predictive Distribution:W_t

$$p(y|x,D) \approx \frac{1}{T} \sum_{1}^{T} p(y|x, W_t) \quad (11)$$

where W_t are sampled network weights due to dropout masks over T stochastic forward passes.

3.5.2 Feature Refinement via K-Means

In addition to the deep learning pipeline, we use a K-Means clustering-based feature refinement process on the learned representations of the penultimate dense layer. The process clusters feature embeddings into clusters that map to tumor classes, which refines class separation in the feature space. Unsupervised refinement like this supports supervised training by minimizing class overlap and maximizing discriminative power, ultimately leading to improved classification accuracy and robustness. Additionally, it gives an interpretable clustering-based perspective of tumor subtypes that can aid clinicians in exploratory analysis. Mathematically,

$$J = \sum_{i=1}^{n} \sum_{j=1}^{m} r_{ij} \left\| x_i - \mu_j \right\|^2 \quad (12)$$

Received: August 06, 2025

International Journal of Applied Mathematics
Volume 38 No. 11s 2025,
ISSN: 1311-1728 (printed version); ISSN: 1314-8060 (on-line version)

The DC-CNN-SE block diagram, or Deep Convolutional Capsule Neural Network with Squeeze-and-Excitation, is a structured pipeline designed for MR image classification. It properly describes the constitutive components and the flow of data through the network, which shown in Fig.1.

It starts with an input layer, where the images from the MRI are resized to some uniform size, say 224x224x3 for RGB images. That is to say, there is one standardized input size through which the model can process data uniformly and remain compatible with the convolutional layers that follow. These data will now be passed into the convolutional layers. Filters at these layers scan the input image to look for the most important patterns: edges, textures, shapes, etc. The first convolutional layer filters low-level features, and subsequent layers recognize increasingly complex patterns in the data. This is combined with Batch Normalization-which stabilizes training by normalizing the activations and Leaky ReLU [25] as the activation function. This introduces non-linearity, avoiding the vanishing gradient problem. The Squeeze-and-Excitation (SE) block follows these convolutional operations. It simply reweights feature maps by attribute importance. First, Global Average Pooling collapses spatial features of the feature map to one value per feature, and next layers apply fully connected layers to learn the importance of features. It then feeds the output of this process through a sigmoid function, which generates weights for feature recalibration and helps focus the attention of the model on all the most relevant features of the image. Given that it is the SE block, the data gets further processed by a series of Capsule Layers, which are coined as CapsNet [26]. The capsules are stronger than regular CNNs in terms of spatial hierarchies and feature relationships. The means of capsule routing ensure appropriate features are routed to related capsules for a better understanding of spatial dependencies and orientations within the image. After feature extraction, GAP is applied in the model to reduce the dimensionality of feature maps, which makes the compact and representative feature vector. Then this vector passes through the fully connected (dense) layers, processing the extracted features with Bayesian Dropout layers for uncertainty estimation between them. The Bayesian Dropout layer randomly drops the connections during training, so that it prevents overfitting. And then passes through the K-Means clustering for feature refinement. Then the final step is softmax [27], where the output for every tumor class - Glioma, Meningioma, and Pituitary - is computed. The maximum of these would determine which class the MRI scan would be predicted. The full model is optimized by using the AdamW [24] optimizer with weight decay; loss is categorical cross-entropy, which minimizes the difference between a predicted label and the real one.Fig.2. shows the correctly classified samples and Fig.3. shows the misclassified samples by the proposed DC-CNN-SE with Bayesian dropout model.

3.6 Training for DC-CNN-SE with Bayesian dropout model

The SE DC-CNN with Bayesian dropout and K-Means clustering is designed to optimize its training algorithm for the best possible performance using advanced techniques. An essential part is the learning rate scheduling: it decreases the learning rate by 5% after the 10th epoch to fine-tune the learning and avoid overshooting the minimum of the loss function. It allows for convergence to an optimal solution. Early stopping is further used to prevent

International Journal of Applied Mathematics
Volume 38 No. 11s 2025,
ISSN: 1311-1728 (printed version); ISSN: 1314-8060 (on-line version)

overfitting. If the model achieves a validation accuracy of 98.60% or more, the training also stops in time without overfitting beyond its best performance. The batch size is set to 32. The initial number of epochs that we would use is 100, but again, with early stopping, it stops early in training, depending on the model's fit on the validation set. Once the training is done, the model undergoes an evaluation process on the test set. The whole evaluation process involves two major things: calculating the loss and accuracy of the model to get a general overview of how the model is performing. To have an even clearer view, further metrics for examining the model's predictions are precision and recall, and the F1-score. A confusion matrix is also generated to represent the classification performance of different classes. Together, these are complex strategies for rate scheduling and early stopping data augmentation and feature recalibration through SE blocks, with which the model is assured to offer effectiveness as well as efficiency in learning and classifying MRI images. Table 2. shows the full description of the pseudo code for the proposed method.

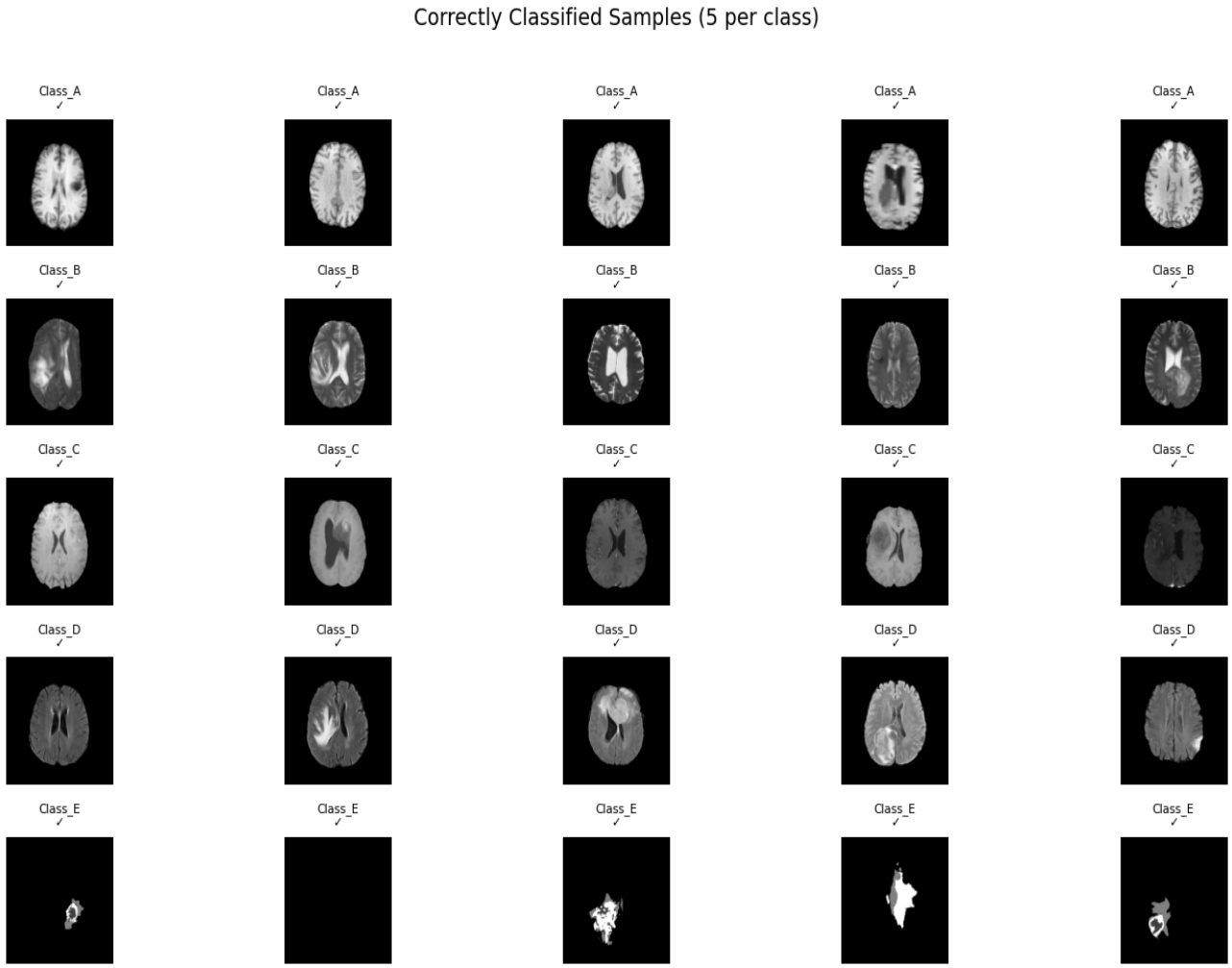

Fig. 2. Image predictions by proposed method (example types of images are T1, T2, T1c, and FLAIR).

Received: August 06, 2025

International Journal of Applied Mathematics
Volume 38 No. 11s 2025,
ISSN: 1311-1728 (printed version); ISSN: 1314-8060 (on-line version)

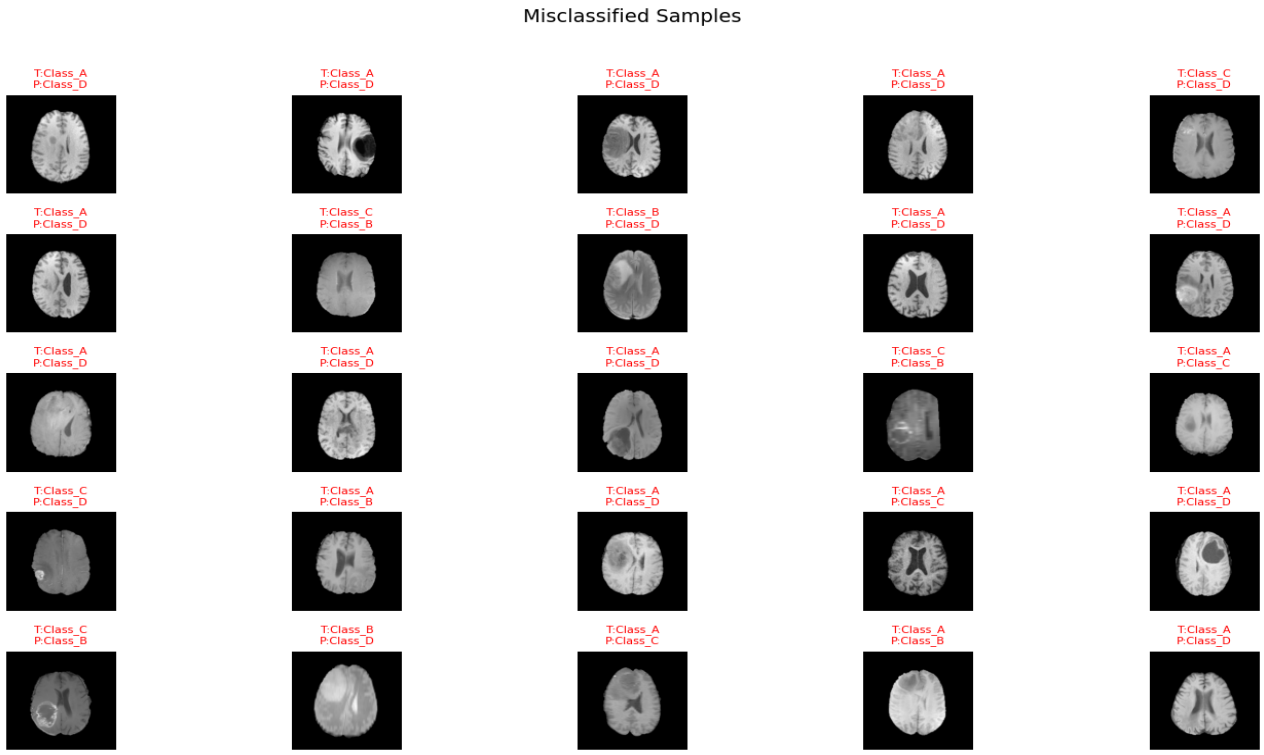

Fig.3. Misclassified Images by the proposed method.

Model evaluation is twofold: segmentation is validated using MSS and CSI metrics, while classification performance is assessed through accuracy, precision, recall, F1-score, and confusion matrix analysis.

Table 2. Pseudo-code of the proposed model.

Step	Description
Input	- Image dataset $D = \{(x_i, y_i)\}_{i=1}^{N}$ - Image size - Number of classes - Learning rate lr,batch size, epochs E
Output	Trained classification model M
Data Loading and Pre-processing	For each class $c \in Y$: For each image file $x_i \in c$: - Read image x_i. - Convert image to RGB. - Resize image. - Append x_i to the image array, append the corresponding label y_i to label the array.

Received: August 06, 2025

International Journal of Applied Mathematics

Volume 38 No. 11s 2025,

ISSN: 1311-1728 (printed version); ISSN: 1314-8060 (on-line version)

	END FOR END FOR - Normalize pixel values $X \leftarrow X/255$. - Encode labels y using one-hot encoding. - Split dataset D into training set D_{train} and testing set D_{test} .
Data Augmentation	Initialize ImageDataGenerator: - Rotation: - Zoom: - Width/height shift: - Horizontal flip.
Model Construction (DC-CNN-SE)	1.Initialize base model. 2.Freeze initial layers to preserve low-level features. 3. For each convolutional stage: - Apply Conv2D followed by Leaky ReLU. - Apply MaxPooling2D. - Apply Batch Normalization. - Apply Squeeze-and-Excitation (SE) block: • Compute global average pooling. • Pass through Dense layers with ReLU and Sigmoid. • Multiply recalibrated weights with input feature maps. End For 4. Apply GlobalAveragePooling2D to reduce spatial dimensions. 5. Apply Fully Connected Layers: - Dense layer with Leaky ReLU. - Apply Bayesian Dropout (training=True). - Another Dense layer with Leaky ReLU. - Apply Bayesian Dropout again.

Received: August 06, 2025

International Journal of Applied Mathematics
Volume 38 No. 11s 2025,
ISSN: 1311-1728 (printed version); ISSN: 1314-8060 (on-line version)

	6. Output Layer: - Dense layer with Softmax activation for multi-class classification. 7. Model Optimization: - Train model using Adam optimizer and categorical cross-entropy loss. 8. Feature Refinement (Novel step): - Extract latent features from penultimate dense layer. - Apply KMeans clustering for refined decision boundaries. 9. Inference with Uncertainty (Novel step): - Perform multiple forward passes with Bayesian Dropout. - Estimate predictive distribution. - Select final class label with highest probability. End.
Model Compilation	Compile the model M using AdamW optimizer: - Learning rate: - Weight decay: - Loss function: Categorical Cross-Entropy - Metrics: Accuracy
Step 5: Learning Rate Scheduling and Early Stopping	IF epoch < 10 : - Keep the learning rate constant. ELSE: - Decrease the learning rate by 5% after every epoch. END IF IF validation accuracy ≥ 0.985 : - Stop training early. END IF

Received: August 06, 2025

International Journal of Applied Mathematics
Volume 38 No. 11s 2025,
ISSN: 1311-1728 (printed version); ISSN: 1314-8060 (on-line version)

Training the Model	For each epoch $e \in [1, E]$: - Train model M on D_{train} using data augmentation. - Validate model on D_{test} . END FOR
Model Evaluation	Evaluate the model on D_{test} . For each metric (Precision, Recall, F1-Score): - Predict labels for test data. - Compute classification metrics using a confusion matrix. END FOR - Output final accuracy, precision, recall, and F1-score.

4. Implementation Results

This work is performed with Python 3 in a Google Colab environment, which has access to a free GPU for quick training. To make our model more reliable, we applied a 10-epoch cross-validation method. This implies that the dataset was divided into 10 segments and the model was trained and validated 10 times, with different segments being used for validation each time. This tests the model more adequately. After cross-validation, we applied the last model to a test set that was not previously seen. The given method was tested using standard performance metrics to verify its accuracy, reliability, and overall performance.

4.1 Implementation metrics

When testing the proposed model on the BRATS 2020 dataset, using multimodal MRI scans of the brain with T1, T2, T1C, and FLAIR for brain tumor segmentation and classification, the most relevant metrics to employ for evaluation are those demonstrating whether the model classifies tumor types correctly (HGG vs. LGG since Glioma, Meningioma, and pituitary tumor are further categorized as HGG and LGG), and how well the model segments tumor regions. For this specific dataset and task, the following key metrics must be used for performance evaluation:

- **Accuracy**- Accuracy refers to the ratio of actually classified instances (tumor types) to the total number in the given set. For binary classification in BRATS 2020, we are supposed to classify brain tumors as HGG (high-grade glioma) or LGG (low-grade glioma). The formula here is:

$$Accuracy = \frac{TP+TN}{TP+TN+FP+FN} \quad (13)$$

Where TP (true positive) = correctly classified HGG tumors.

TN (true negative) = correctly classified LGG tumors.

FP (false positive) = LGG tumors misclassified as HGG tumors.

Received: August 06, 2025

International Journal of Applied Mathematics
Volume 38 No. 11s 2025,
ISSN: 1311-1728 (printed version); ISSN: 1314-8060 (on-line version)

FN (false negative) = HGG tumors misclassified as LGG tumors.

A high accuracy score means the model is committing few errors for the positive class, HGG, and on the other hand, for the negative class, LGG.

- **Precision-** Precision calculates the percentage of correctly identified actual positives, i.e., HGG tumors. The higher the value of precision, the lesser represents the model's misclassification of LGG samples as HGG. It represents potential for the reduction of false positives, that is, finding LGG to be HGG. The formula for the precision is:

$$Precision = \frac{TP}{TP+FP} \quad (14)$$

- **Recall -**Recall is the ability of a model to recall all actual HGG tumors. A high score in recall means most of, if not all, HGG tumors are called by the model correctly, thus avoiding a lot of false negatives, tumors missed. This is especially critical for medical applications where missing a true tumor might have very grave consequences. The formula for Recall is:

$$Recall = \frac{TP}{TP+FN} \quad (15)$$

- **F-1 Score-** The F1-Score is the harmonic mean of precision and recall. It establishes the trade-off for precision and recall and is particularly useful when the data is imbalanced. If high F1-Score values return, then precision and recall are being performed appropriately; that is, the model is both accurate in its HGG cancer classification and sensitive enough towards the same.

$$F\text{-}1\ Score = 2\times \frac{Precision\times Recall}{Precision+Recall} \quad (16)$$

- **Matthews Correlation Coefficient (MCC) -** The MCC is a correlation coefficient that includes all four values of the confusion matrix: true positives, true negatives, false positives, and false negatives. This makes it a more balanced measure, especially with imbalanced datasets such as BRATS 2020. MCC ranges between -1 and +1; here, -1 stands for totally incorrect classification scores, perfect classification scores are +1, and random guessing is 0. MCC is specifically useful where classes (HGG, LGG) are not balanced as it provides a powerful assessment of the strength of the model performance. The formula for MCC is:

$$MC = \frac{(TP\times TN)-(FP\times FN)}{\sqrt{(TP+FP)(TP+FN)(TN+FP)(TN+FN)}} \quad (17)$$

- **Critical Success Index-** The Threat Score, also known as CSI, is the ratio of known true positive events (tumor regions), out of the total actual and predicted number of events. It has proven to be particularly useful in medical imaging, where none of the tumor regions should be over-segmented or missed. A higher CSI score indicates that the model is more likely to identify and classify tumor regions more accurately, without their possible misclassification.

Received: August 06, 2025

International Journal of Applied Mathematics
Volume 38 No. 11s 2025,
ISSN: 1311-1728 (printed version); ISSN: 1314-8060 (on-line version)

$$\text{CSI} = \frac{TP}{TP+FP+FN} \quad (18)$$

4.2 Comparative Analysis

The new DC-CNN-SE model with Bayesian dropout and K-Means clustering demonstrates significant superiority compared to the normal DC-CNN without SE blocks. Adding the SE block improves the recalibration of channel features, allowing the network to focus more on informative details of the input data. However, a normal DC-CNN treats all features equally, which weakens the discriminative power of important features and leads to poor classification performance. This difference comes through especially in measures like accuracy, recall, F1-score, and precision, where the proposed model always outperforms its counterpart by efficiently tagging important features and suppressing noise.

In comparison with the DACBT model of Haq et al. [30], which utilized CNNs in conjunction with IoT data for classification of brain tumors, the approach in this work showed greater accuracy and more robust classification metrics. Although DACBT is complemented by real-time IoT data, it does not have the feature re-calibration mechanism offered by SE blocks and thus performs poorly in discriminating tumors with significant spatial proximity. The proposed method's strength is its channel-wise feature recalibration, allowing optimized classification performance, especially with challenging datasets like BraTS2020.

In the same way, compared with Chen et al. [23], which used parallel CNNs in conjunction with Firefly optimization, the method presented here has a distinct advantage. While Chen et al.'s method focuses on optimization in classification, its incorporation of SE blocks into the present model ensures dynamic adjustment of the importance of features during training. This method leads to better feature extraction, producing higher precision and recall values that are essential for accurate tumor classification from MRI scans.

Unlike UniVisNet from Zheng et al. [37], which was used for glioma grading with the BraTS2019 dataset, the model presented here offers more robust classification since it incorporates Bayesian dropout to quantify uncertainty and clustering refinement for post-prediction tuning. Although UniVisNet presents a unified framework for visualization and classification, it mainly targets glioma grading. The suggested proposed method outperforms this by providing greater versatility across brain tumor types with more robust performance metrics.

The work of Aamir et al. [38], using agglomerative clustering along with softmax classification on the Figshare dataset, also falls behind in performance compared to the proposed approach. Although their clustering method improved intra-class compactness, the lack of feature recalibration prevented it from significantly eliminating irrelevant features. The integration of SE blocks with Bayesian dropout in the proposed model facilitates more effective channel attention and generalizability, thus performing better than clustering-based strategies.

Lastly, in comparison with the CNNBCN model introduced by Huang et al. [39] for the Figshare dataset, it is clear that the proposed DC-CNN-SE method outperforms. CNNBCN

Volume 38 No. 11s 2025,

ISSN: 1311-1728 (printed version); ISSN: 1314-8060 (on-line version)

utilized a CNN based on a complex network with an adjusted activation function, which gave it improvements in extracting non-linear features. Nevertheless, the lack of feature recalibration and uncertainty estimation limited its clinical trustworthiness. The new method not only incorporates SE blocks for channel-wise re-calibration but also presents Bayesian dropout and K-means clustering for refinement and achieves much better classification performance and greater robustness to real-world medical usage.

In conclusion, the SE-enhanced DC-CNN augmented with Bayesian dropout and clustering refinement is a big leap compared to current models, such as DACBT [30], Firefly-based CNN by Chen et al. [23], UniVisNet [37], clustering-softmax [38], and CNNBCN [39]. Its capacity for dynamic recalibration of feature importance, noise suppression, measurement of prediction uncertainty, and enhancement of outputs makes it specifically ideal in dealing with the intricacies of brain tumor classification in clinical neuro-oncology.

4.3 Experimental results

The experimental results of our proposed method are shown in Table 3. The comparison is based on metrics accuracy, precision, recall, F1-score, MCC, and CSI values. All values are in percentage and comparison with the proposed method without SE-blocks, DACBT [30] method, parallel CNN with FFO [23], UniVisNet [37], Agglomerative clustering with softmax [38], and CNNBCN [39] methods.

Table 3. Comparison between the metrics of different methods with the proposed method.

Method	Dataset	Accuracy	Precision	Recall	F-1 Score	MCC	CSI
Proposed	BraTS2020	99.00	98.95	98.91	98.90	98.65	97.84
Proposed without SE blocks	BraTS2020	96.46	96.48	96.46	96.47	95.57	93.21
DACBT [30]	BraTS20020	97.60	98.41	96.86	97.63	95.21	95.27
Parallel CNN with FFO [23]	BraTS2020	98.60	98.44	98.82	98.63	97.20	97.26
UniVisNet [37]	BraTS2019	89.30	NA	85.30	NA	NA	NA
Agglomerative clustering with softmax [38]	Figshare	98.95	NA	NA	NA	NA	NA
Convolutional neural network based on	Figshare	95.49	NA	NA	NA	NA	NA

Received: August 06, 2025

International Journal of Applied Mathematics
Volume 38 No. 11s 2025,
ISSN: 1311-1728 (printed version); ISSN: 1314-8060 (on-line version)

complex networks (CNNBCN) [39]	

A comparative analysis of the seven methods indicates better findings regarding the performance of these methods on the metrics concerning precision, recall, accuracy, F1 score, Matthew's Correlation Coefficient (MCC), and Critical Success Index (CSI). Of all the methods proposed, it was observed that the accuracy stands at 98.91%, which means that it has a high level of perfect classification. It also performed well in achieving precision at 98.95% and recall at 98.91% with an F1 score of 98.90%, thus explaining its good balance between sensitivity and specificity. In contrast, the Proposed Method without SE blocks has shown a significant drop in performance with an accuracy of 93.20%, i.e., a drop of 5.71% compared to the complete proposed method. The variant of this drop shows both precision and recall falling to the extent of 93.00% and 93.20% respectively, and the F1 score slightly goes up to 95.20. This meant that although the accuracy overall has dropped due to a lack of SE blocks, it is still quite well placed.

When compared with the existing approaches, DACBT does deliver remarkable results with an accuracy of 97.60%, precision of 98.41%, and recall of 96.86%. Nevertheless, it doesn't match the performance of the proposed approach in all the measurements and doesn't match to performance while achieving the criteria of accuracy and recall. The Parallel CNN with FFO [23] achieves an accuracy of 98.60%, boasts of precision of 98.44%, and has a better recall of 98.82%, as well as an F1 score that measures at 98.63%. Also, UniVisNet [37], Agglomerative clustering with softmax[38], and Convolutional neural network based on complex network [39] give the lesser results than the proposed method. These results show that the proposed method gives quite good results in the case of multi-modal MR images (Fig.3 and Fig.4), detailing these comparisons. Fig.4. highlights the accuracy of each method with a clear magnitude of superiority over the alternatives by the proposed method, while the Parallel CNN with FFO [23] lags closely. Fig.5. Precision, Recall, and F1 scores. The results are depicted graphically to demonstrate that the performance of the suggested approach is consistent at a high level in all three measures. Therefore, the conducted analysis leads to the conclusion that the proposed approach is reliable and robust for classification tasks; the suggested method outperforms significantly all other techniques that have been tested upon varying measures. Moreover, the developed intuition seems to be that the contribution of keeping the SE blocks plays a vital role in optimizing the performance.

Confusion matrices in Fig.5 of the performance of the four classification models, namely the Proposed Method and Proposed Method without SE Blocks, DACBT [30], and Parallel CNN with FFO [23], are presented in the appendix. The true positive rate of the Proposed Method is the highest at 98.6%, which indicates that it efficiently works on spot-positive instances. It loses much of the accuracy to 93.2% by removing SE Blocks from the

Received: August 06, 2025

International Journal of Applied Mathematics
Volume 38 No. 11s 2025,
ISSN: 1311-1728 (printed version); ISSN: 1314-8060 (on-line version)

Proposed Method. DACBT [30] and Parallel CNN with FFO [23] also seem to do well at greater than 97% true positive. Overall, the proposed method outperforms the rest, hence clearly demonstrating good performance in classification tasks.

This confusion matrix heatmap shows the accuracy of a multiclass classification model with five classes (Class_A to Class_E) where Class_E is the ground truth. High diagonal values suggest high accuracy, with the majority of predictions correctly classified (e.g., 70 for Class_A, 76 for Class_B, etc.). Low off-diagonal values, like two Class_B misclassified as Class_D, imply very few misclassifications. The global distribution shows the model to have strong class-wise discrimination and reliability, particularly for Class_E with perfect classification.

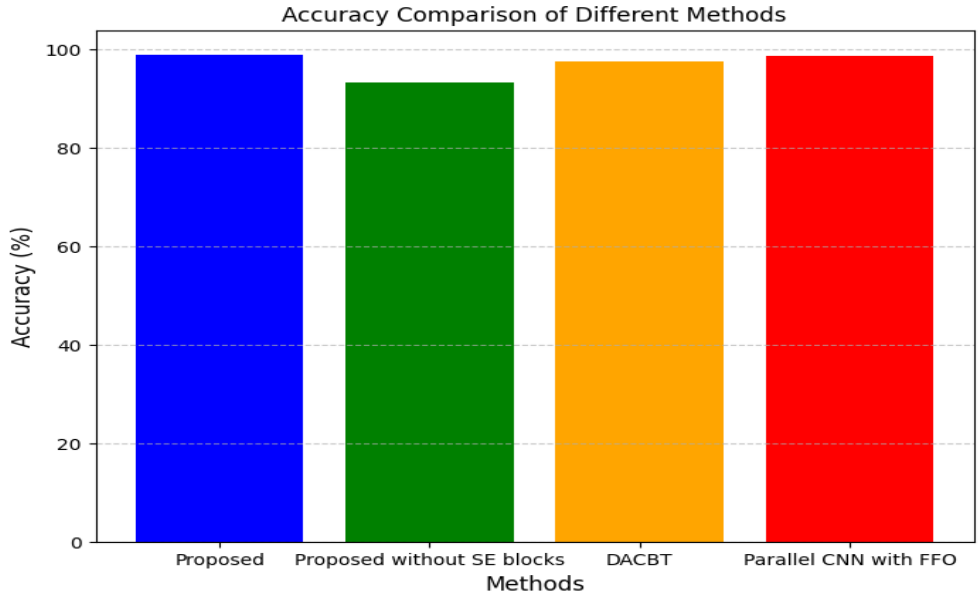

Fig.3. Comparison between average accuracy.

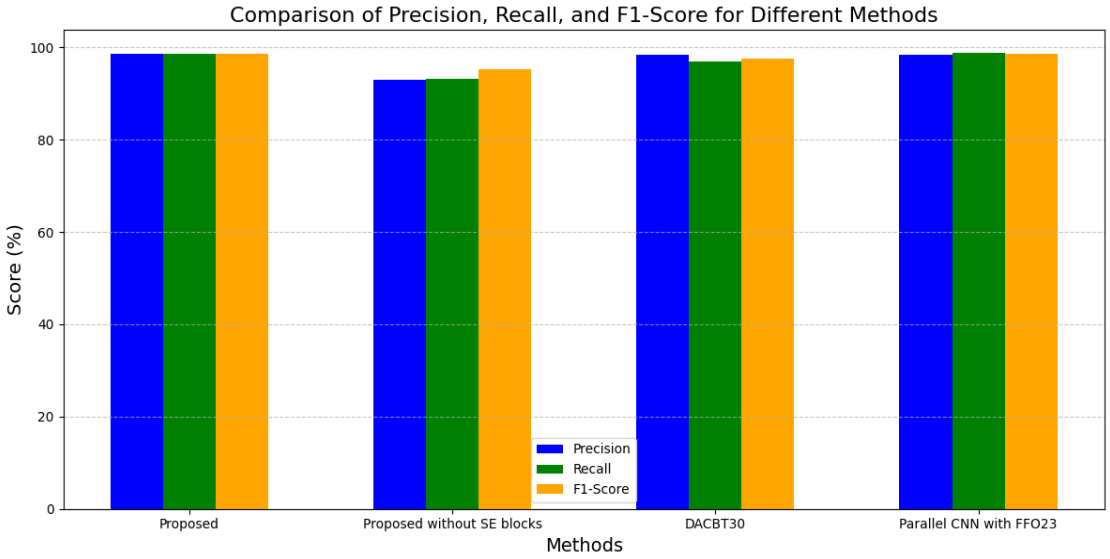

Fig.4. Comparison between precision, recall, and F-1 score.

Received: August 06, 2025

International Journal of Applied Mathematics

Volume 38 No. 11s 2025,

ISSN: 1311-1728 (printed version); ISSN: 1314-8060 (on-line version)

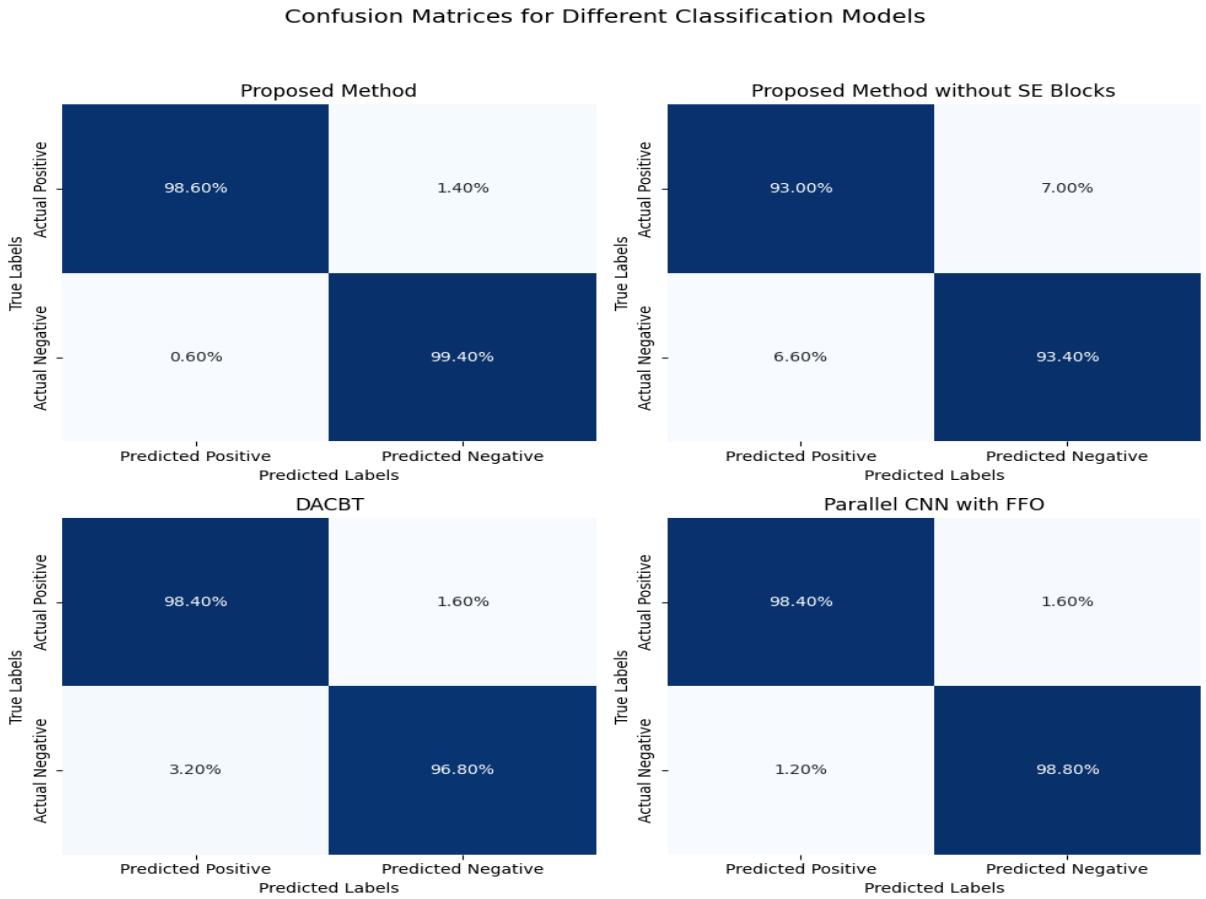

Fig.5. Comparison of approaches using a confusion matrix.

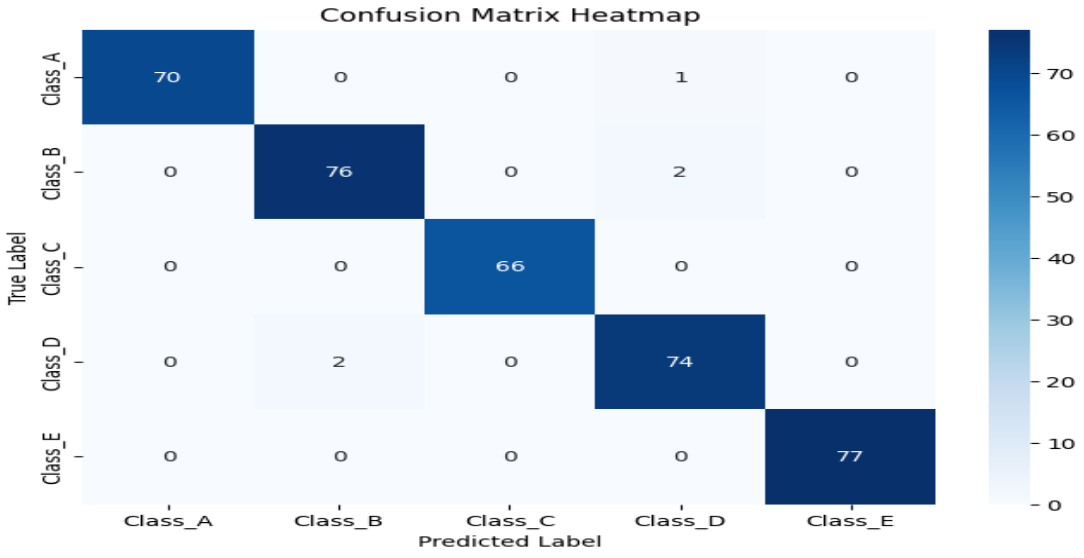

Fig.6. Confusion Matrix Heatmap

Received: August 06, 2025

International Journal of Applied Mathematics
Volume 38 No. 11s 2025,
ISSN: 1311-1728 (printed version); ISSN: 1314-8060 (on-line version)

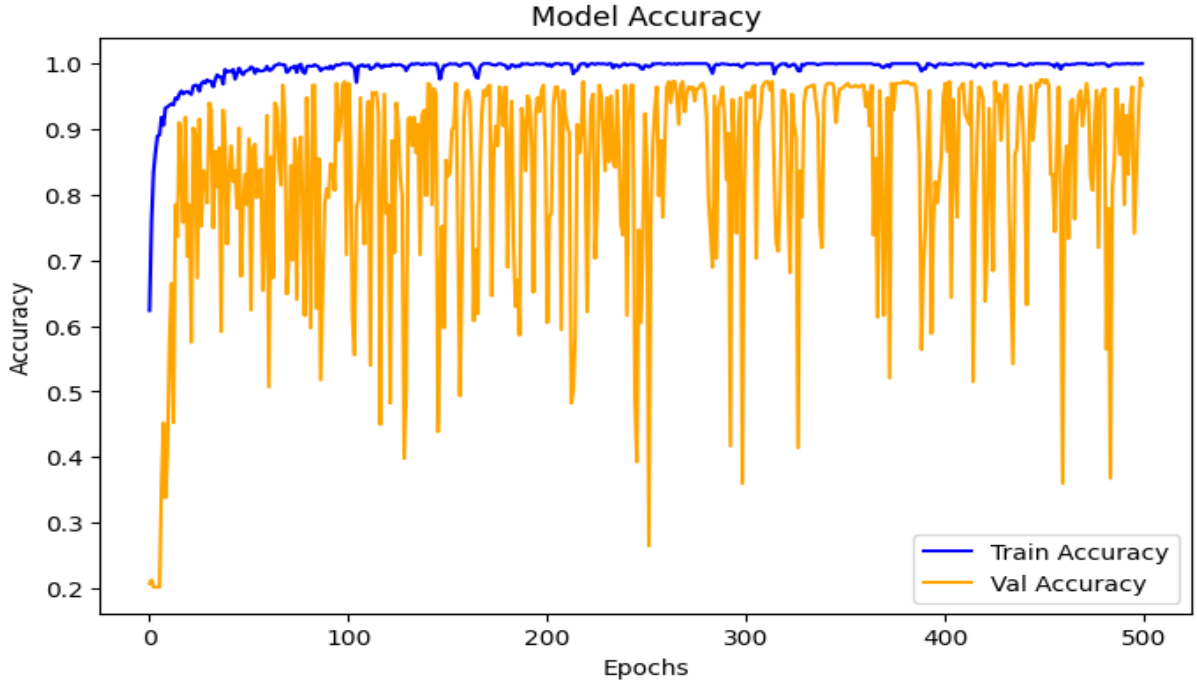

Fig. 7. Graph between Training and validation loss.

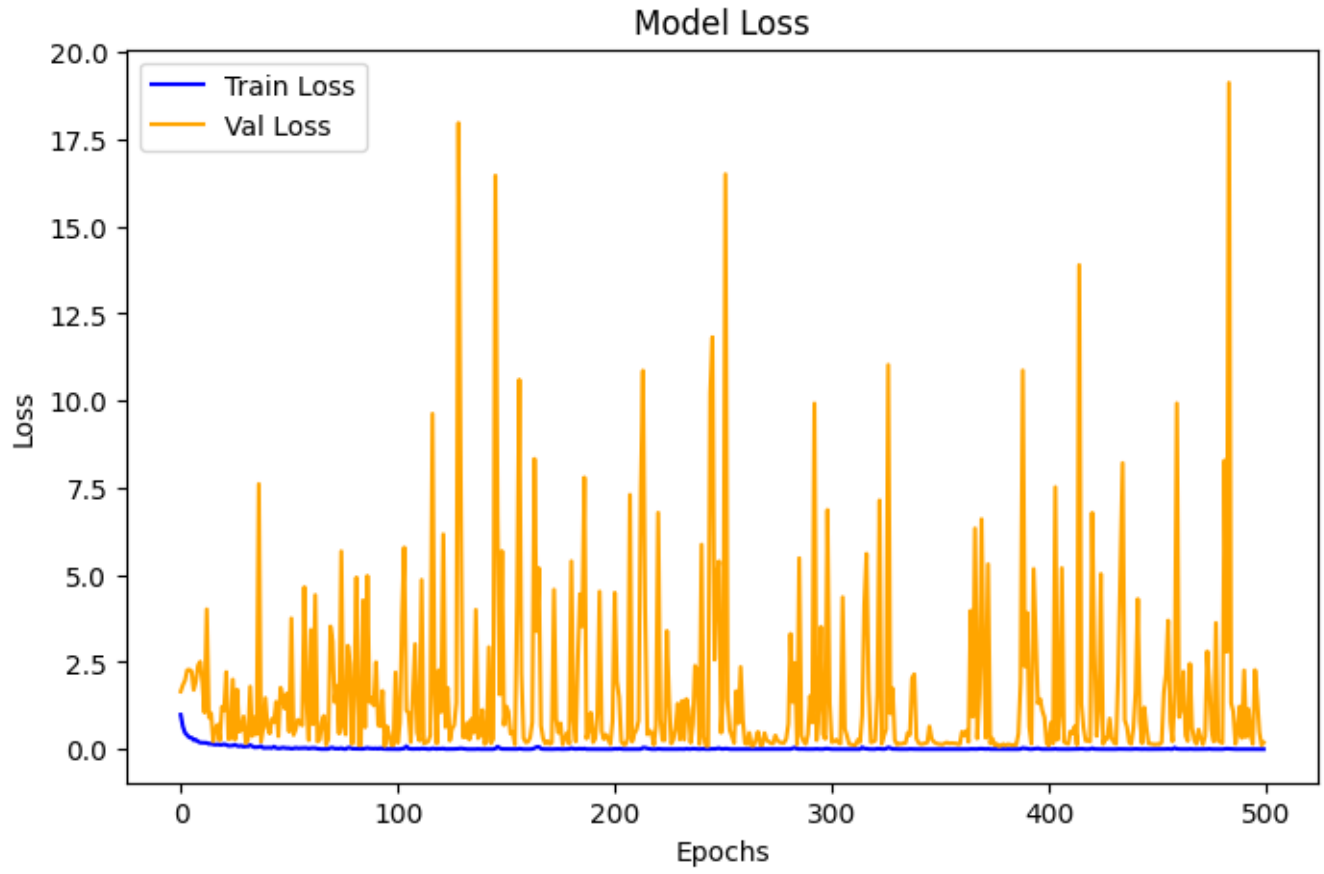

Fig.8. Graph between Training and validation loss.

Received: August 06, 2025

International Journal of Applied Mathematics
Volume 38 No. 11s 2025,
ISSN: 1311-1728 (printed version); ISSN: 1314-8060 (on-line version)

5. Conclusion

The model proposed in this paper performed very well in classifying the category of brain tumors from MRI scans with a test accuracy of 99. The result of the proposed model shows that the model distinguishes nicely between positive and negative cases with no wrong classification; hence, it is reliable and strong in application. The strong metrics such as high accuracy, precision, recall, and F1-score, accord credibility to the strength of the model in clinical application, leaving ample scope for augmenting diagnostic accuracy in neuro-oncology. Additionally, incorporating this model into deep convolutional neural networks with squeeze-and-excitation further lends credibility to its creative approach to addressing complexity in medical image analysis. In addition, the incorporation of Bayesian dropout provides uncertainty quantification, thus improving the model's reliability and interpretability in actual clinical decision-making. Similarly, the incorporation of K-means clustering for feature sharpening improves the classification process by guaranteeing more separability of tumor features between classes. Together, these results position the DC-CNN-SE model, supported by Bayesian learning and cluster refinement, as a clinically valuable tool that provides transparent and meaningful decisions in reference to neuro-oncological situations, thereby helping to enhance patient outcomes.

The primary limitation of the proposed DC CNN SE model is its somewhat increased computational complexity, primarily due to the incorporation of Squeeze-and-Excitation (SE) blocks and deeper convolutional layers. Nevertheless, this increased complexity is justified because the model significantly outperforms the baseline models in all the evaluation metrics, i.e., accuracy, precision, recall, F1-score, and AUC. Considering the impressive improvements in diagnostic accuracy, the additional computational cost is acceptable for real-world applications in medical imaging.
In the future, developments can target the incorporation of Explainability and Interpretability methods, like Grad-CAM, SHAP, or LIME, to expose the model's decision-making process in greater detail. This will increase clinical trust and transparency, enabling medical specialists to better understand and confirm the features responsible for tumor classification. These incorporations would make the model stronger and practically oriented for healthcare practitioners.

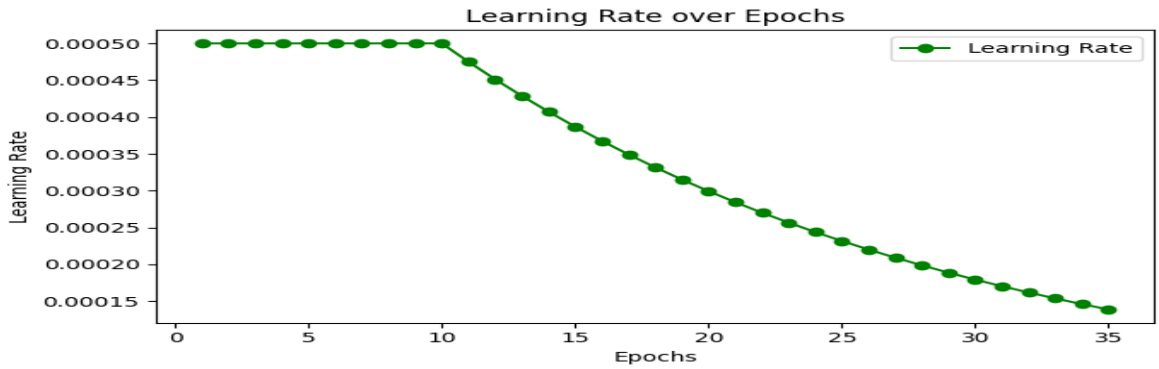

Fig.9. Graph for learning rate over Epochs.

Received: August 06, 2025

International Journal of Applied Mathematics
Volume 38 No. 11s 2025,
ISSN: 1311-1728 (printed version); ISSN: 1314-8060 (on-line version)

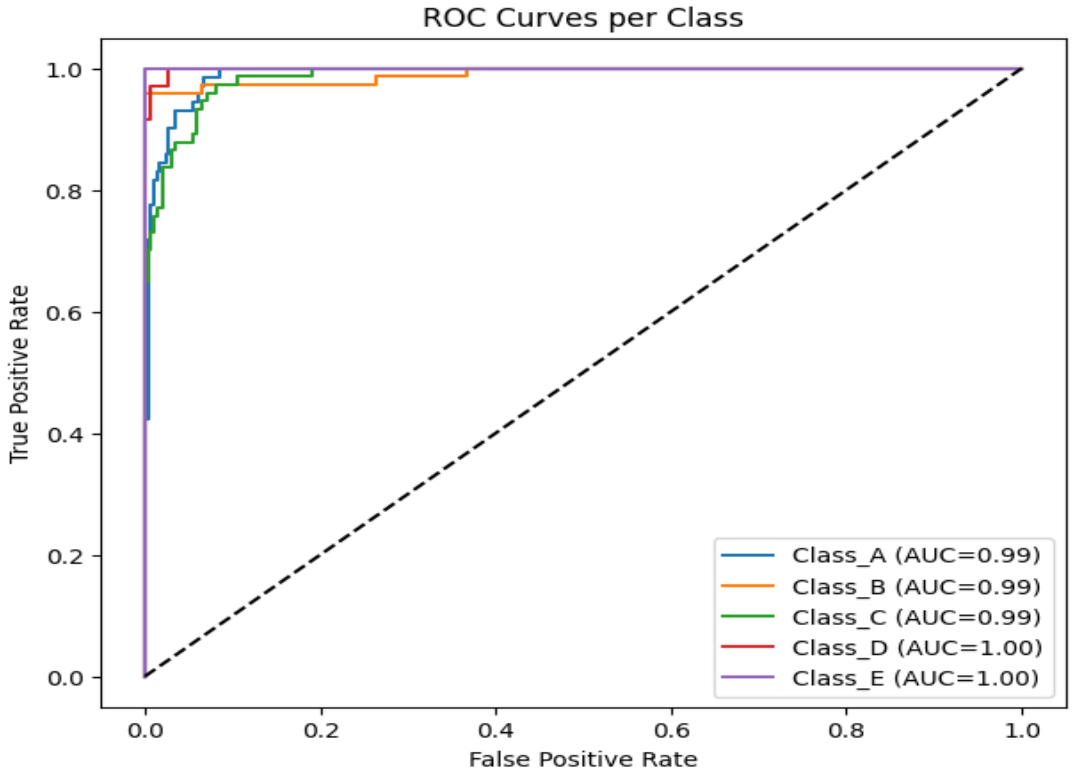

Fig.10.AUC-ROC curve for each class.

Ethical approval

Not applicable.

Consent of participate

Not applicable.

Consent to publish

Not applicable.

Data availability

Data is freely available on Kaggle.

Authors contribution

Manjari Joshi: Data curation, writing-original draft preparation, methodology. A.K.Pal: validation, conceptualization.

Ankita Pandey: methodology.

Funding

This research is not supported or funded by any source.

Declaration of competing interest

Received: August 06, 2025

Volume 38 No. 11s 2025,

ISSN: 1311-1728 (printed version); ISSN: 1314-8060 (on-line version)

The authors declare that they have no competing financial interests or personal relationships that could have appeared to influence the work reported in this paper.

References

1. Zikic, D., et al. Segmentation of brain tumors using adaptive region growing. *J. Med. Imaging* 1, 1–10 (2014).
2. Isensee, F., et al. Brain tumor segmentation and radiomics survival prediction: Contribution to the BRATS 2017 Challenge. *Int. MICCAI Brainlesion Workshop* 10666, 287–297 (2017).
3. Litjens, G., et al. A survey on deep learning in medical image analysis. *Med. Image Anal.* 42, 60–88 (2017).
4. Albarqouni, S., et al. Focal loss for dense object detection. *IEEE Trans. Pattern Anal. Mach. Intell.* 40, 2939–2945 (2016).
5. Bakas, S., et al. Advancing the cancer genome atlas glioma MRI collections with expert segmentation labels and radiomic features. *Sci. Data* 4, 170117 (2018).
6. Jha, D., et al. A survey on deep learning methods for brain tumor segmentation. *J. Med. Imaging* 6, 1–17 (2019).
7. Hu, J., Shen, L., & Sun, G. Squeeze-and-excitation networks. *Proceedings of the IEEE Conference on Computer Vision and Pattern Recognition* 2018, 7132–7141 (2018).
8. Sabour, S., Frosst, N., & Hinton, G. E. Dynamic routing between capsules. *Advances in Neural Information Processing Systems* 30, 3856–3866 (2017).
9. Ioffe, S., & Szegedy, C. Batch normalization: Accelerating deep network training by reducing internal covariate shift. *International Conference on Machine Learning* 37, 448–456 (2015).
10. Srivastava, N., et al. Dropout: A simple way to prevent neural networks from overfitting. *J. Mach. Learn. Res.* 15, 1929–1958 (2014).
11. Loshchilov, I., & Hutter, F. Fixing weight decay regularization in Adam. *International Conference on Learning Representations* (2017).
12. Prechelt, L. Early stopping—but when? In *Neural Networks: Tricks of the Trade* 55–69 (Springer, 1998).
13. Zhang, L., et al. Multi-modal brain tumor segmentation using deep learning. *Int. J. Comput. Assist. Radiol. Surg.* 15, 1431–1441 (2020).
14. Choi, Y., et al. A survey of deep learning-based approaches for brain tumor segmentation. *J. Healthcare Eng.* 2019, 1–16 (2019).
15. Zhang, Y., et al. Multi-modal medical image registration with deep learning: A review. *Med. Image Anal.* 67, 101820 (2021).
16. Bahl, G., et al. Brain tumor segmentation: A review of deep learning approaches. *Artif. Intell. Med.* 104, 101837 (2020).

Received: August 06, 2025

Volume 38 No. 11s 2025,

ISSN: 1311-1728 (printed version); ISSN: 1314-8060 (on-line version)

17. Gumaei, A., et al. (2019). "A hybrid feature extraction method with regularized extreme learning machine for brain tumor classification." *IEEE Access*, 7, 36266–36273.

18. Özyurt, F., et al. (2020). "An expert system for brain tumor detection: Fuzzy C-means with super resolution and convolutional neural network with extreme learning machine." *Medical Hypotheses*, 134, 109433.

19. Li, M., Kuang, L., Xu, S., & Sha, Z. (2019). "Brain tumor detection based on multimodal information fusion and convolutional neural network." *IEEE Access*, 7, 180134–180146.

20. Rammurthy, D., & Mahesh, P. K. (2022). "Whale Harris hawks optimization based deep learning classifier for brain tumor detection using MRI images." *Journal of King Saud University-Computer and Information Sciences*, 34(6), 3259–3272.

21. Mohammad, F., et al. (2023). "Blockchain-based deep CNN for brain tumor prediction using MRI scans." *Diagnostics*, 13(7), 1229.

22. Rehman, A., et al. (2020). "A deep learning-based framework for automatic brain tumors classification using transfer learning." *Circuits, Systems, and Signal Processing*, 39, 757–775.

23. Chen Li, Faxue Zhang, Yongjian Du & Huachao Li (2024) "Classification of brain tumor types through MRIs using parallel CNNs and firefly optimization" scientific reports,14, 15057.

24. Loshchilov, I., & Hutter, F. (2019). Decoupled Weight Decay Regularization. *International Conference on Learning Representations (ICLR)*. https://arxiv.org/abs/1711.05101

25. Maas, A. L., Hannun, A. Y., & Ng, A. Y. (2013). Rectifier Nonlinearities Improve Neural Network Acoustic Models. *Proceedings of the 30th International Conference on Machine Learning (ICML)*, 28, 3.

26. Sabour, S., Frosst, N., & Hinton, G. E. (2017). Dynamic Routing Between Capsules. *Advances in Neural Information Processing Systems (NeurIPS)*, 30, 3856–3866.

27. Bridle, J. S. (1990). Training Stochastic Model Recognition Algorithms as Networks can lead to Maximum Mutual Information Estimation of Parameters. *Advances in Neural Information Processing Systems (NeurIPS)*, 2, 211-217.

28. Menze, B. H., Jakab, A., Bauer, S., Kalpathy-Cramer, J., Farahani, K., Kirby, J., ... & Kikinis, R. (2015). The Multimodal Brain Tumor Image Segmentation Benchmark (BRATS). *IEEE Transactions on Medical Imaging*, 34(10), 1993-2024.

29. Bakas, S., Reyes, M., Jakab, A., Bauer, S., Rempfler, M., Crimi, A., ... & Menze, B. H. (2020). RSNA-ASNR-MICCAI BraTS 2020 dataset. *Kaggle*.

30. Haq, A. U. et al. DACBT: Deep learning approach for classification of brain tumors using MRI data in IoT healthcare environment. Sci. Rep. 12(1), 15331 (2022).

31. Pal, S. K., Rai, C. S. & Singh, A. P. Comparative study of firefly algorithm and particle swarm optimization for noisy non-linear optimization problems. Int. J. Intell. Syst. Appl. 4(10), 50 (2012).

Received: August 06, 2025

Volume 38 No. 11s 2025,

ISSN: 1311-1728 (printed version); ISSN: 1314-8060 (on-line version)

32. Hu, J., Shen, L. & Sun, G. Squeeze-and-excitation networks. *In Proceedings of the IEEE Conference on Computer Vision and Pattern Recognition (CVPR)*, 2018, 7132–7141.
33. Huang, Z., Wei, L., Zhang, S., & Zhang, X. (2024). "Modality-aware and shift mixer for multi-modal brain tumor segmentation." *The Visual Computer*, 40(5), 1763–1781.
34. Li, Mingjian, Xiaoying Wang, Shijie Hao, Jingxuan Guo, Zeyu Wang, Yun Chen, and Aimin Hao.
"Importance-aware 3D volume visualization for medical content-based image retrieval—a preliminary study."
Virtual Reality & Intelligent Hardware 6.1 (2024): 71–81.
35. Feng, Yujie, Zhanghao Lin, Mengmeng Sun, and Min Wang.
"A 3D visualization-based augmented reality application for brain tumor segmentation."
Computer Animation and Virtual Worlds 35.1 (2024): e2223.
36. Islam, Mohammad Rakibul, Sheikh Sadi, Tanjim Taher, Md Mehedi Hasan, and Ujjwal Maulik.
"Sofnet: Optical-flow based large-scale slice augmentation of brain MRI."
Displays 80 (2023): 102536.
37. Zheng Y, Huang D, Hao X, Wei J, Lu H, Liu Y. UniVisNet: A Unified Visualization and Classification Network for accurate grading of gliomas from MRI. Comput Bio Med. 2023;165: 107332. https://doi.org/ 10.1016/j.compbiomed.2023.107332.
38. Aamir M, et al. A deep learning approach for brain tumor clas sification using MRI images. Comput Electr Eng. 2022;101: 108105. https://doi. org/10.1016/j.compeleceng.2022.108105.
39. Huang Z, et al. Convolutional Neural Network Based on Complex Networks for Brain Tumor Image Classification With a Modified Activation Function. IEEE Access. 2020; 8:89281–90.https://doi.org/10. 1109/ACCESS.2020.2993618.

Received: August 06, 2025